

OBSERVATION AND SIMULATION OF TSUNAMIS INDUCED BY THE 2003 TOKACHI-OKI EARTHQUAKE (M 8.0)

Tatsuo Ohmachi*¹, Shusaku Inoue¹, and Tetsuji Imai²

¹Department of Built Environment, Tokyo Institute of Technology, Japan

²Civil Engineer, Tokyo Gas Company, Ltd., Japan

Abstract

The 2003 Tokachi-oki earthquake (MJ 8.0) occurred off the southeastern coast of Tokachi, Japan, and generated a large tsunami which arrived at Tokachi Harbor at 04:56 with a wave height of 4.3 m. Japan Marine Science and Technology Center (JAMSTEC) recovered records of water pressure and sea-bed acceleration at the bottom of the tsunami source region. These records are first introduced with some findings from Fourier analysis and band-pass filter analysis. Water pressure disturbance lasted for over 30 minutes and the duration was longer than those of accelerations. Predominant periods of the pressure looked like those excited by Rayleigh waves. Next, numerical simulation was conducted using the dynamic tsunami simulation technique able to represent generation and propagation of Rayleigh wave and tsunami, with a satisfactory result showing validity and usefulness of this technique.

Keywords: Earthquake, Rayleigh wave. tsunami, near-field.

1 Introduction

About a decade ago, the dynamic tsunami simulation technique was developed by Ohmachi et al. (2001a) to simulate the generation of tsunamis followed by their propagation. It takes into account not only the dynamic displacement of the seabed induced by seismic

faulting but also the acoustic effects of the seawater. As the dynamic technique assumes weak coupling between the seabed and seawater, the simulation consists of a two-step analysis. The first is on the dynamic seabed displacement resulting from seismic faulting, and the second is on the seawater disturbance induced by the dynamic seabed displacement. In the first step, the boundary element method (BEM) is used. In the second, the finite difference method (FDM) is used to solve the Navier-Stokes equation. A series of dynamic tsunami simulations have demonstrated that in the near-field of tsunami sources there are some significant differences from those resulting from conventional technique because water waves associated with water compressibility and dynamic sea surface disturbance are not accounted in the latter technique.

Although the features from the dynamic analysis seems quite reasonable, they have to be verified by observed data (Ohmachi et al. 2001b). For this reason, the data obtained by JAMSTEC (Japan Marine Science and Technology Center) during the 2003 Tokachi-oki earthquake and the dynamic tsunami simulation are used in the present study.

2 The 2003 Tokachi-oki earthquake and offshore monitoring system

The 2003 Tokachi-oki earthquake of magnitude 8.0 occurred off the southeastern coast of Tokachi at 04:50 on September 26, 2003. Report-

*Corresponding author: T. OHMACHI, Department of Built Environment, Tokyo Institute of Technology, Japan. E-mail: ohmachi@enveng.titech.ac.jp

edly, the tsunami arrived at Tokachi Harbor at 04:56 with a wave height of 4.3 m, while the Japanese Nationwide Coastal Wave Observation Network (NOWPHAS) located on the 23m-deep seabed off Ohtsu Harbor recorded the first tsunami arrival at 04:51 (Nagai and Ogawa 2004). The locations of these harbors and epicenter of the earthquake are shown in Figure 1, where the location of the offshore monitoring system deployed by JAMSTEC and a fault model dipping northwest (Koketsu *et al.* 2004) are also shown. The system is equipped with 3 sets of 3-component broadband seismometers (OBS1-3) and 2 high-precision pressure gauges (PG1-2). The distances between OBS1 and PG1 and between OBS3 and PG2 are 4.0 km and 3.4 km, respectively. As these two pairs are nearly located, the locations of these pairs are referred to as St. A and St. B in Figure 1, and the distance between these two stations is about 72 km. Table 1 shows elements of the offshore monitoring system and seawater depth at each sensor (JAMSTEC 2009). Sampling rates of the pressure gauges and seismometers are 1 Hz and 100 Hz, respectively.

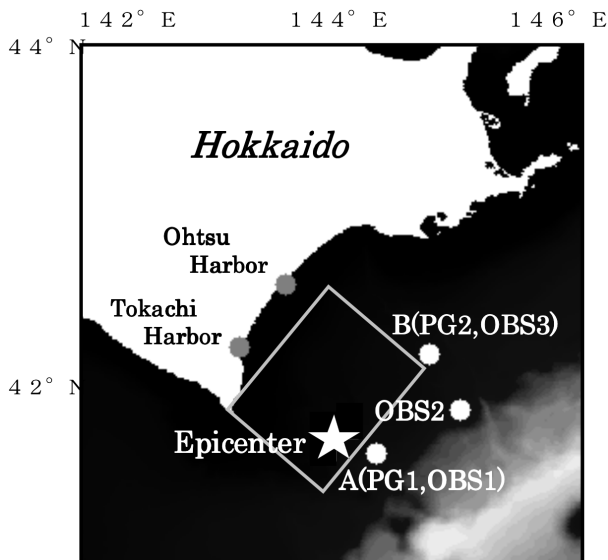


Figure 1: Locations of the JAMSTEC monitoring system equipment and epicenter of the 2003 Tokachi-oki earthquake.

Table 1: The JAMSTEC offshore monitoring system and water depth of equipment.

3 Tsunami generation process inferred from observed data

Time histories of water pressure and ground motion acceleration (vertical component) at St. A and St. B are shown in Figure 2. Apparently, the water pressure change lasted longer than the ground motion acceleration. Fourier spectra of the time histories are shown in Figure 3. Peak periods of 7.0 s at St. A and 6.5 s at St. B are observed in both water pressure and ground motion acceleration, and each period T can be approximated by $T=4H/c$, where $H(=2.2 - 2.3 \text{ km})$ is the seawater depth and $c(=1.5 \text{ km/s})$ is an acoustic wave velocity of water (Nosov *et al.* 2005).

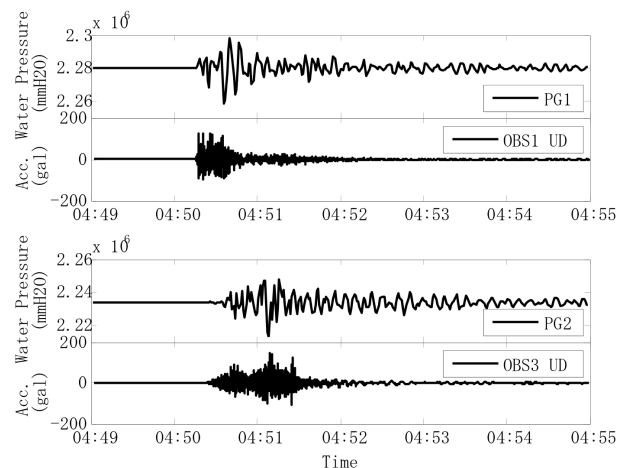


Figure 2: Time histories of water pressure and vertical ground motion acceleration.

Time histories of the water pressure change in Figure 2 are full of short period components with amplitudes several times larger than the tsunami-induced water pressure. When the period components shorter than 50s are filtered out, the water pressure time histories result in those indicated by the gray curves in Figure 4. It is interesting to note that after the main shock, the baseline of the water pressure was shifted by about 40 cm at PG1 and about 10 cm at PG2 in terms of the water depth. These baseline shifts were supposedly caused by the uplift of

OBSERVATION AND SIMULATION OF TSUNAMIS INDUCED BY THE 2003 TOKACHI-OKI EARTHQUAKE

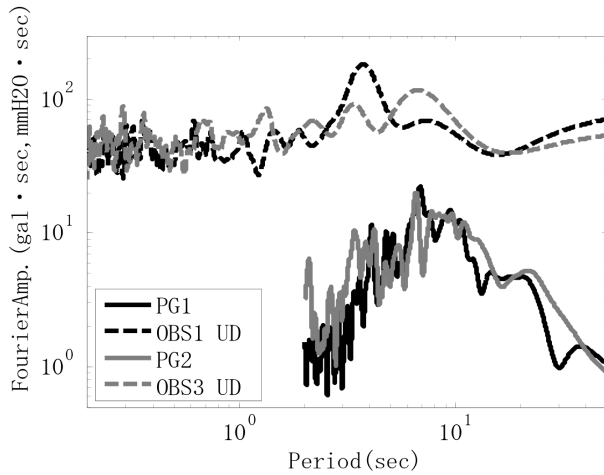


Figure 3: Fourier spectra of time histories shown in Figure 2.

the seabed due to the seismic faulting (Watanabe et al. 2004).

The gray curves in Figure 4 indicate the shape of the recently-generated tsunami. At PG2, the tsunami looks like a solitary wave with a height of about 20 cm and a period of 15 min. At PG1, the wave height and the period are not so clear as those at PG2, and a gentle slope only can be observed. The difference in the shape of the tsunami is due to the difference in the relative location between the observation stations and the tsunami source.

In addition, the gray curves indicate another group of water waves preceding the tsunami at the beginning of the short-period water pressure change which are referred to be preceding waves.

4 Water waves induced by Rayleigh waves

Band-pass filtering between 3s and 15s was applied to the original time histories of water pressure and vertical ground motion displacement at St. A and St. B, with the result shown in Figure 5. It can be seen that the water pressure change in this period range had the largest amplitude at the beginning of the earthquake motion as the seabed displacement occurred. Figure 6 shows the particle orbit of the ground motion displacement plotted on the vertical NS-UD plane during 4:50:20 and 4:50:40. During

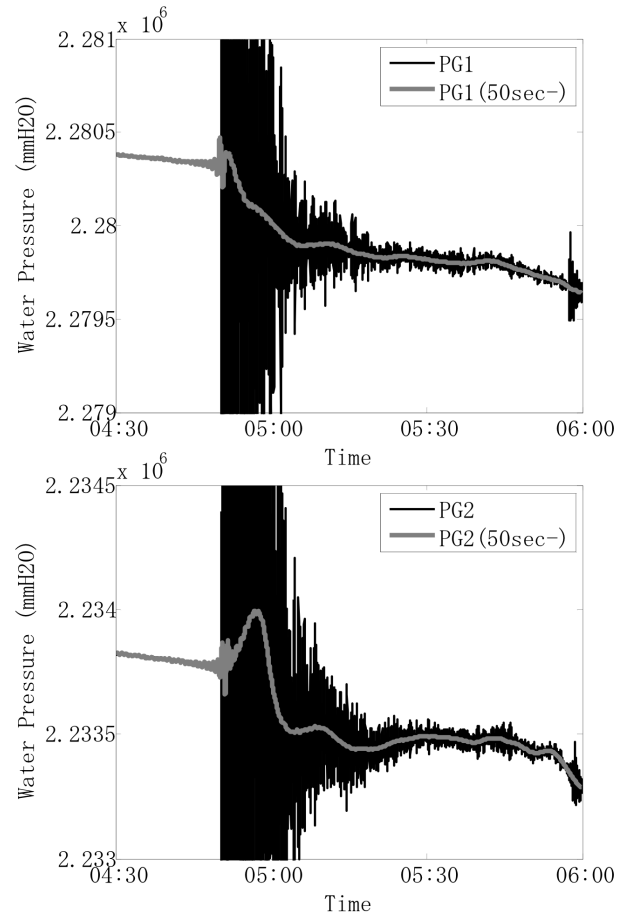


Figure 4: Time histories of water pressure after long-pass filtering of 50 s.

the 20s, the particle orbit showed an elliptic retrograde motion but not so clear on the EW-UD plane, which suggests the directionality of the wave motion. From the particle motion and the directionality, the motion is considered to be mainly due to Rayleigh waves.

Propagation of vertical ground displacements associated with the 2003 earthquake is illustrated in Figure 7, which was obtained from double integration of acceleration time histories observed at K-net stations in and around Hokkaido. Large amplitude arrived at the southeast coast of Hokkaido at about 20s and propagated in the northwestern direction. The waves are probably due to Rayleigh waves with the wave length of about 100 km and wave velocity of about 3.5 km/s.

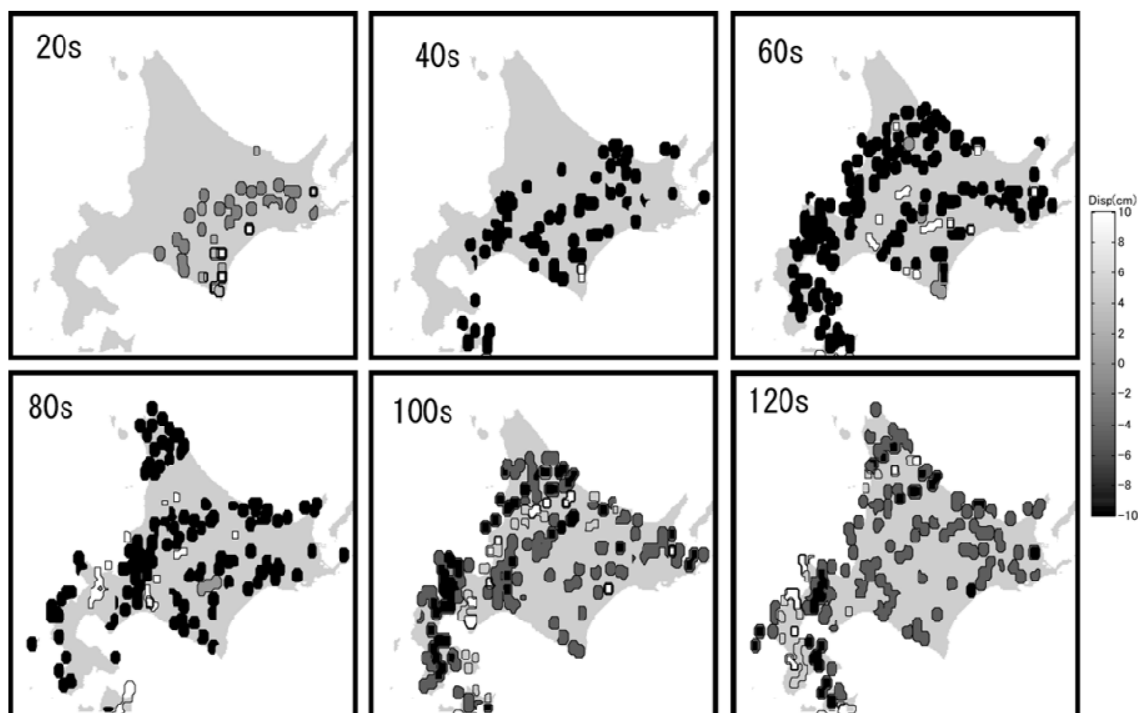


Figure 7: Observed ground displacement of UD-component at K-net

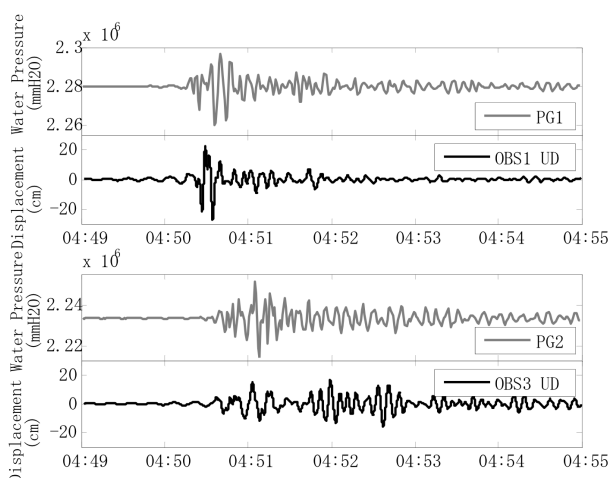


Figure 5: Time histories of water pressure and vertical ground motion displacement after band-pass filtering of 3-15 s

5 Tsunami simulation

A fault model proposed by Koketsu *et al.* (2004) is used in this simulation (see Figure 1). The area of the simulation is 250 km long in the NS direction and 350 km wide in the EW direction. The grid size for the seabed and water

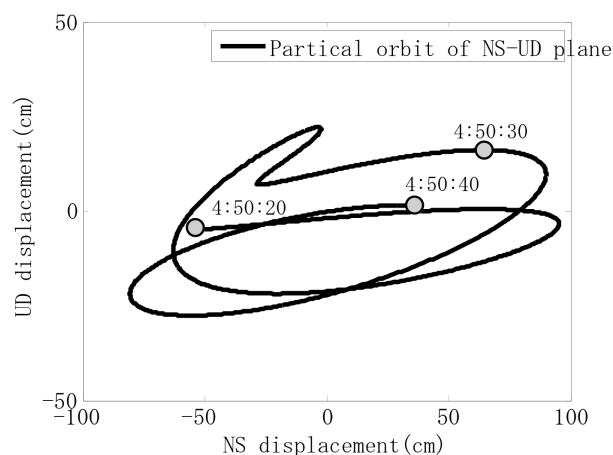


Figure 6: Particle orbit of ground motion displacement at OBS1 during 04:50:20 and 04:50:40.

layer is 5km and 1km, respectively. Fault rupture starts at the southeastern edge and extends to the northwestern direction with a velocity of 3km/s. The total duration of the fault rupturing is about 30s.

Snapshots in Figures 8 and 9 show the simulation results. At 20s the faulting progresses up to the middle of the fault plane. From 60s to 80s,

the water wave induced by the Rayleigh wave is propagated to the northwestern coast. At 80s when the fault rupture finishes, static uplift and subsidence remain in the near-fault area and the tsunami profile is almost the same as that of the static displacement of the seabed.

The dynamic simulation technique can deal with not only the tsunami generation but also the water wave induced by Rayleigh waves which was actually observed before the tsunami arrival.

6 Conclusions

Analysis of the JAMSTEC monitoring data have shown that three kinds of water waves were involved in the dynamic tsunami generation process following the 2003 Tokachi-oki earthquake; that is, water pressure waves of short period, a tsunami of long period, and preceding waves of intermediate period.

As for the tsunami of long period, two types of recently generated tsunamis were detected by the water pressure gauges. One was a solitary wave with a height of about 20 cm and a period of 15 min, and the other had a gentle slope and its wave height and period were not so clear as the first type. The first type was detected at a station located a little distant from the seismic fault, while the second was detected at a station just above the fault plane. The water waves preceding the tsunami were detected in an early stage of the water pressure change and they were seemingly induced by a large seabed displacement associated with the Rayleigh waves because of the directivity, an elliptical particle orbit, and a predominant period ranging between 3 s and 15 s.

These three kinds of water waves can be analyzed by the dynamic simulation technique.

Further studies are needed for early detection and warning of near-field tsunamis, especially on the dynamic process of the tsunami generation, using both observation and simulation as shown in the present paper.

Acknowledgements

The authors are grateful to JAMSTEC for the data from the deep-sea monitoring used in this study.

References

- JAMSTEC (2009), "Submarine Cable Data Center," <http://www.jamstec.go.jp/scdc/> K. Koketsu, K. Hikima, S. Miyazaki and S. Ide (2004), "Joint inversion of strong motion and geodetic data for the source process of the 2003 Tokachi-oki, Hokkaido, earthquake," *Earth Planets Space*, 56(3), 329-334.
- T. Nagai and H. Ogawa (2004), "Characteristic of the 2003 Tokachi-off Earthquake Tsunami Profile," Technical Note on the Port and Airport Research Institute, No. 1070.
- M. Nosov, S. V. Kolesov, A. V. Ostroukhova, A. B. Alekseev and B. M. Levin (2005), "Elastic oscillations of the water layer in a tsunami source," *Doklady Earth Sciences*, 404(7), 1097-1100.
- T. Ohmachi, H. Tsukiyama and H. Matsumoto (2001a), "Simulation of Tsunami Induced by Dynamic Displacement of Seabed due to Seismic Faulting," *Bull. Seis. Soc. Am.*, 91(6), 1898-1909.
- T. Ohmachi, H. Tsukiyama and H. Matsumoto (2001b), "Sea Water Pressure Induced by Seismic Ground Motions and Tsunamis," *ITS2001*, 595-609 (2001b).
- T. Watanabe, H. Matsumoto, H. Sugioka, H. Mikada and K. Suyehiro (2004), "Offshore Monitoring System Records Recent Earthquake Off Japan's Northernmost Island," *Eos Trans. AGU*, 85(2), doi:10.1029/2004EO020003.

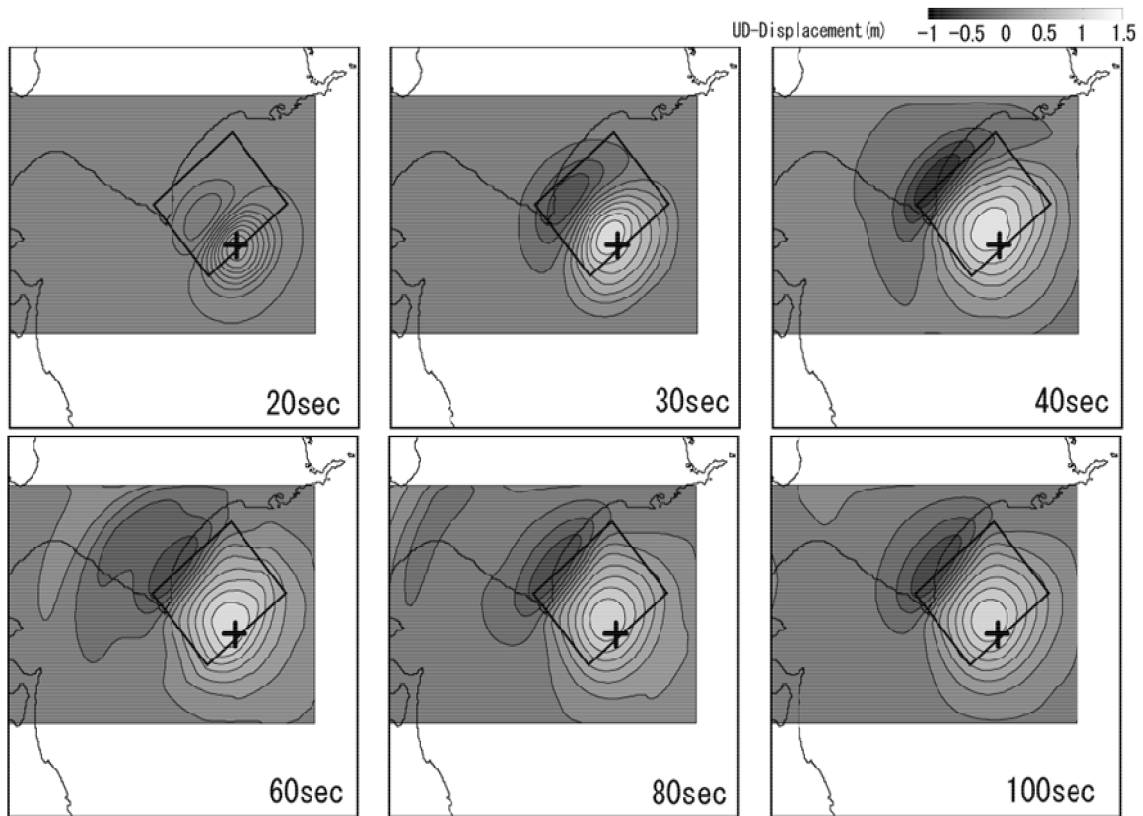


Figure 8: Contour map of simulated vertical displacement of the ground and sea-bed

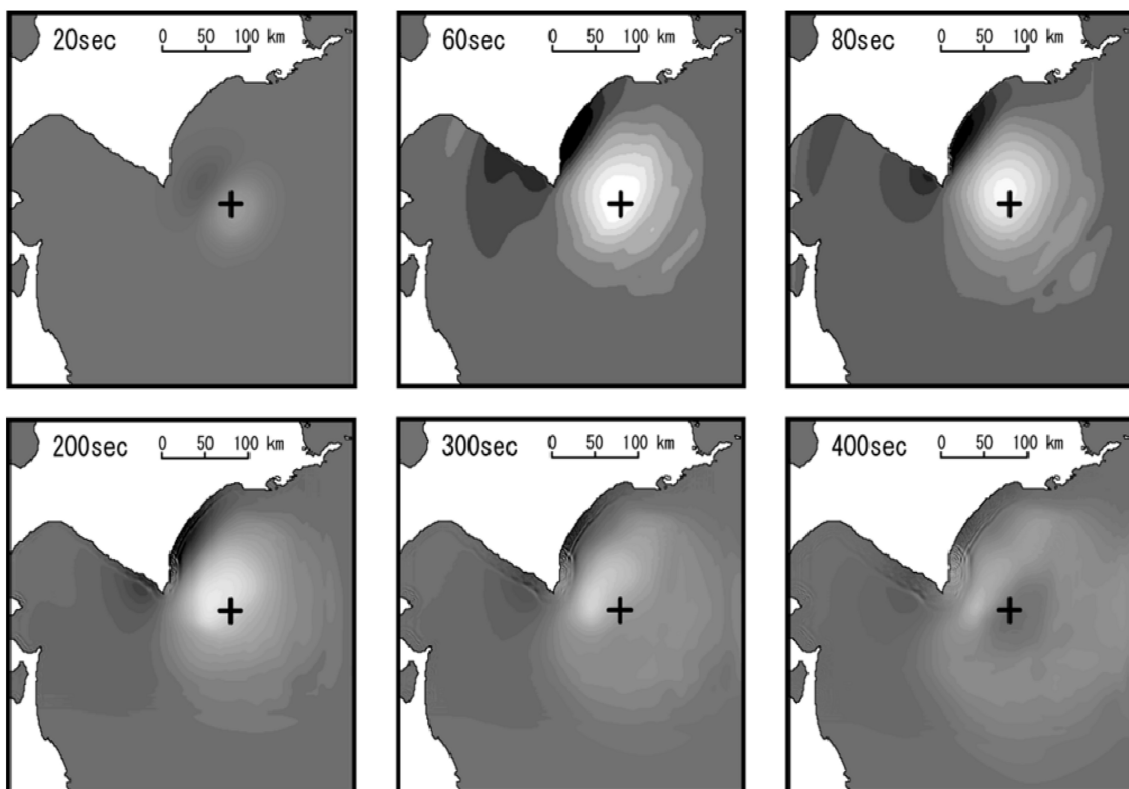


Figure 9: Snapshots of simulated water level